PROCEEDINGS OF THE INTERNATIONAL CONFERENCE
NANOMATERIALS: APPLICATIONS AND PROPERTIES
Vol. **2** No 2, 02PCN21(4pp) (2013)

Thickness Dependent Growth of Epitaxial Iron Silicide Nanoobjects on Si (001)

G. Molnár[1,*], L. Dózsa[†], Z. Vértesy[‡], Zs.J. Horváth[1,2,§]

[1] *Institute of Technical Physics and Materials Science, Research Centre for Natural Sciences, HAS, Budapest, H-1525 P.O. Box 49, Hungary*
[2] *Óbuda University, Kandó Kálmán Faculty of Electrical Engineering, Institute of Microelectronics and Technology, H-1084 Budapest,Tavaszmező u. 15-17, Hungary*

(Received 05 June 2013; published online 31 August 2013)

Strain-induced, self-assembled iron silicide nanostructures were grown on Si(001) substrate by conventional Fe evaporation and subsequent annealing. The initial Fe thickness was in the 0.1-6.0 nm range and the annealing temperature was 850 °C. The formed phases and structures were characterized by reflection high energy electron diffraction, and scanning electron microscopy. The electrical characteristics were investigated by I-V and C-V measurements, and by DLTS. The samples show silicide nanostructure formation in the whole thickness range. The shape of the nanostructures varied from rod like to triangular and quadratic depending on the initial Fe thickness. The size distribution of the formed iron silicide nanoobjects was not homogeneous, but they were oriented in square directions on Si(001). Higher thickness resulted in increased particles size.

Keywords: Iron silicide, Self-assembly, Nanostructures.

PACS numbers: 64.75.Yz, 81.15.Np

1. INTRODUCTION

Future generation thin film solar cells have to use abundantly available, non toxic and environmentally friendly chemical elements. Semiconducting β-$FeSi_2$ is a possible material, which has 23 % theoretical efficiency in solar cells, and both its layer and nanoparticle forms have potential applications in photovoltaic technology [1]. Recently, Terasawa and coworkers proposed a composite β-$FeSi_2$/ Si film for photovoltaic use, where photocarriers generated in the iron silicide particles, which has high photoabsorption coefficient, and photocarrier transport takes place in silicon. This material may result a superior solar cell due to its high photoabsorption coefficient and high carrier mobility [2].

β-$FeSi_2$ is an indirect semiconductor, but in some epitaxial configurations on silicon substrate it has a direct band gap due to strain effects [3, 4]. The following phases of the Fe-Si equilibrium phase diagram have found in thin film reactions, mainly on Si(111) substrates: The most Fe-rich silicide is Fe_3Si (DO_3 type), with cubic structure. Two types of iron monosilicides may appear in thin film form. The first phase is ε-FeSi with cubic structure and the second monosilicide phase is cesium-chloride type cubic FeSi. The iron disilicides, prepared in thin layers, might have three different crystal structures. The high temperature, metastable, tetragonal α-$FeSi_2$ phase may be epitaxially stabilized in thin film form on Si substrates. The cubic γ-$FeSi_2$ phase is also a metastable structure. At the end, β-$FeSi_2$ has orthorhombic structure. All of the above phases, including metastable ones, may be epitaxially stabilized on the surface of Si substrates [5].

The fabrication of artificial low dimensional structures is one of the most challenging research fields in the solid state technology. These nanoobjects are prepared by physical and chemical or by combined methods and they have attracted great interest, according to their scientific peculiarity and technical significance. One of the most challenging methods of nanostructure production is the phenomena of self-assembly, that has been applied in case of compound and group IV semiconductors and wide range of material and substrate combinations [6].

In case of self-assembly the natural laws are used as instruments to product nanostructures. The strain induced self-assembled growth is a basic physical method of the preparation of nanostructures. During the growth of strained layers, the film is able to remain planar up to a critical thickness that depends on the lattice mismatch between the film and the substrate. Above a critical thickness, three dimensional, dislocation free islands may form [7]. This phenomenon is known as Stransky-Krastanov transition, which is an important way of the preparation of self-assembled quantum dots and wires.

The motivation of the recent study was to find proper methods for the preparation of iron silicide nanostructures. Actually, we have demonstrative examples of the existence of iron silicide nanostructures [8], but they have not been systematically grown on Si substrates with different initial Fe thicknesses at a same annealing temperature. Research on the above fields may contribute to gain new knowledge in epitaxial growth and morphology changes in iron silicides, and for practical side to prepare more effective solar cells.

* molnar.gyorgy@ttk.mta.hu
† dozsa.laszlo@ttk.mta.hu
‡ vertesy.zofia@ttk.mta.hu
§ horvath.zsolt@kvk.uni-obuda.hu

2. EXPERIMENTAL

Pieces of (001) oriented Si (*p*-type, 12-20 Ω·cm) wafers were used as substrates. Before loading the samples into the oil free evaporation chamber their surface was etched in diluted HF. Prior to evaporation Si wafers were annealed in situ for 5 min at 850 °C. Iron ingots of 99.9 % purity were evaporated using an electron gun, at an evaporation rate of 0.01-0.03 nm/s, at a pressure of $3 \cdot 10^{-6}$ Pa. The film thickness was measured by vibrating quartz. The temperatures were monitored by small-heat-capacity Ni-NiCr thermocouples. The initial Fe thicknesses were in the 0.1-6.0 nm range and the annealing temperature was 850 °C. During evaporation the substrates were held at room temperature (RT) and the subsequent annealings were carried out in situ.

The phases and structures were characterized by reflection high energy electron diffraction (RHEED), scanning- electron microscopy (SEM). The electrical characteristics were investigated by I-V and C-V measurements and the defects were measured by deep level transient spectroscopy (DLTS).

3. RESULTS AND DISCUSSION

During sample preparation the whole process was followed by RHEED. In Fig. 1(a) can be seen the RHEED image taken from the cleaned and annealed Si(001) substrate showing 2×1 reconstruction. The RHEED image of Fig. 1(b) shows state of the surface after 0.1 nm iron evaporation. As can be seen, the original Si surface reconstruction disappeared and the lines weakened, as consequence of very thin Fe covering. After 60 min annealing at 850 ºC according to the RHEED image a new, reconstructed surface developed showing the epitaxial character of the iron silicide (Fig. 1(c))

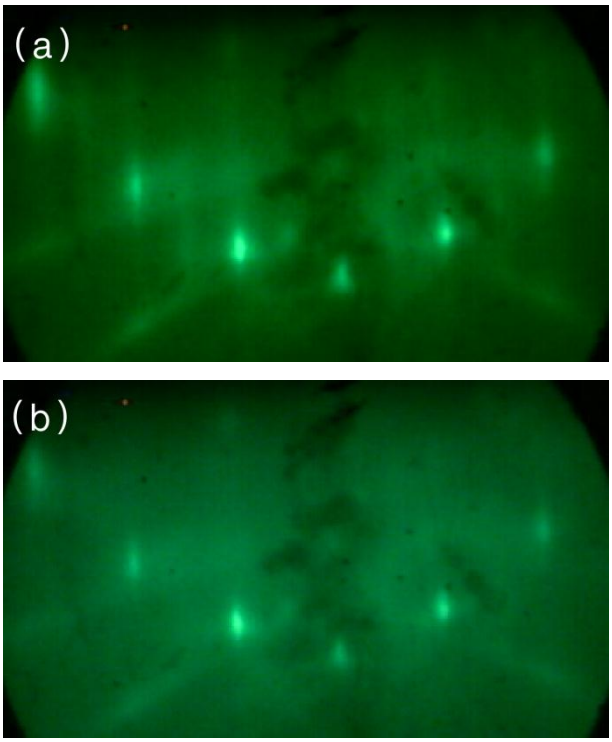

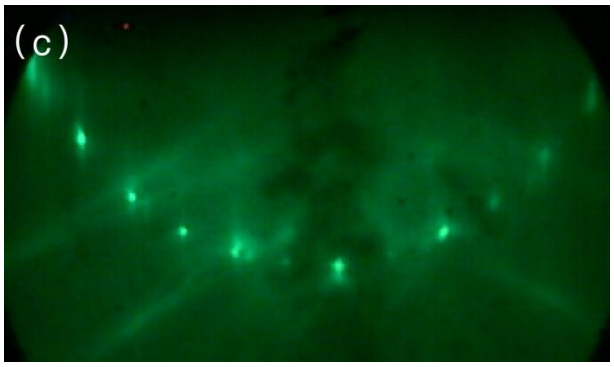

Fig. 1 – RHEED images of (a) the Si(001) substrate, (b) after 0.1 nm iron evaporation, (c) after 60 min annealing at 850 ºC

In case of thicker films in Fig. 2(a) can be seen the RHEED image of the Si(001) substrate. The image of Fig. 2(b) shows the polycrystalline surface after 3 nm iron evaporation. After 60 min annealing at 850 ºC a new, dotted pattern developed showing the epitaxy of the iron silicide (Fig. 2(c)).

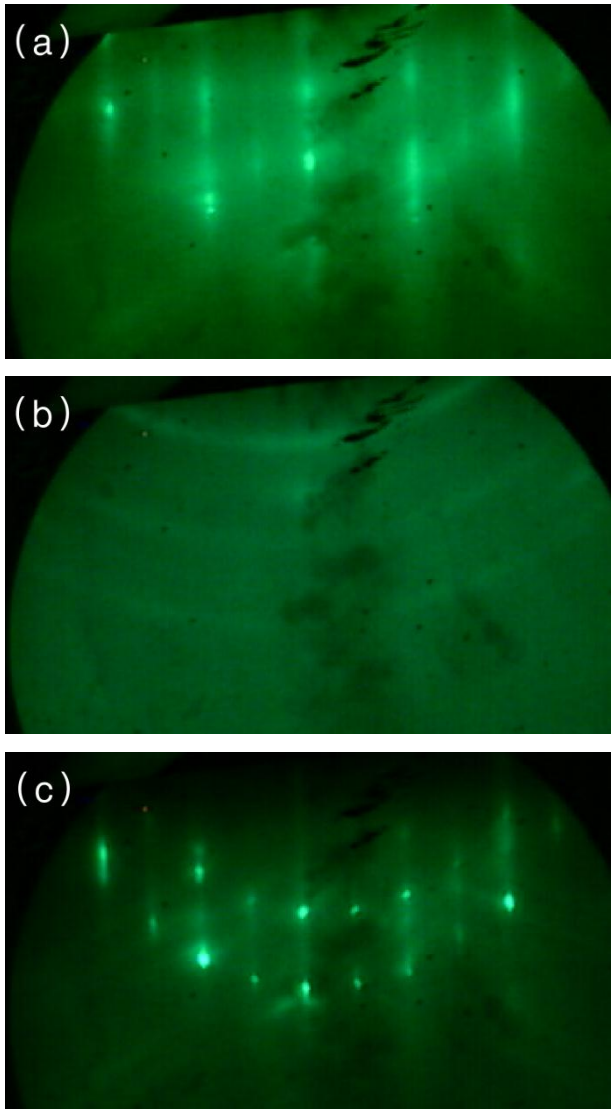

Fig. 2 – RHEED images of (a) the Si(001) substrate, (b) after 3 nm iron evaporation, (c) after 60 min annealing at 850 ºC for iron silicide formation

The scanning electron microscopy investigations present that all of the samples show aggregated iron silicide nanoobjects. The thickness dependence of iron silicide nanostructure formation is shown in Fig. 3. All of the samples were annealed at 850 °C for 60 minutes. The initial mass equivalent iron thicknesses were 0.1, 0.3, 0.6, 1.0, 3.0, and 6.0 nm as are shown Fig. 3(a-e), respectively.

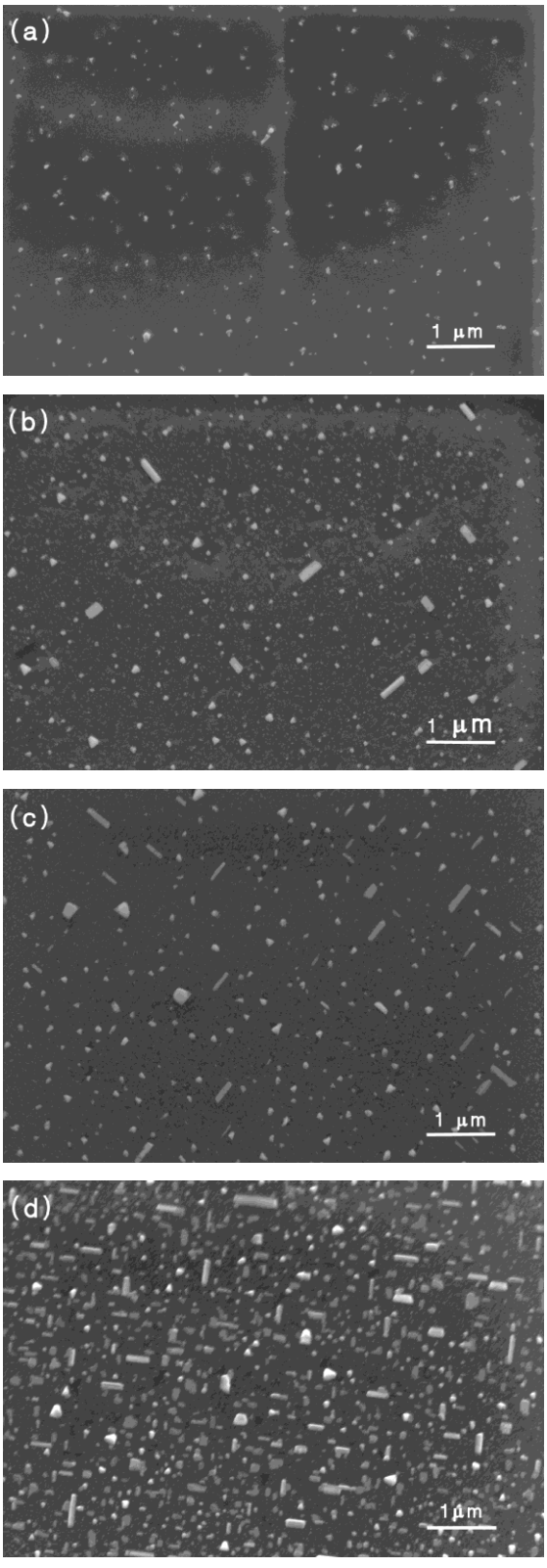

Fig. 3 – SEM images of thickness dependent formation of iron silicides at the same annealing (850 °C, 60 min). The nanoobjects developed from (a) 0.1 nm, (b) 0.3 nm, (c) 0.6 nm, (d) 1.0 nm, (e) 3.0 nm, (f) 6.0 nm initially evaporated iron film

The size and the distribution of the islands depend on the initial Fe thickness. The thicker films resulted in nanostructures with enhanced size, and with decreased density taking into account both the maximum size and the smaller islands too.

These phenomena might be a consequence of Ostwald ripening. In post deposition conditions where no additional material is being deposited, Ostwald ripening is considered the primary coarsening mechanism for island growth [9]. The primary role of the Ostwald ripening is strengthened by the depleted regions around the bigger objects.

Samples that formed from 0.3-1.0 nm Fe show triangular, elongated, and rectangular nanoobjects, which appeared in square directions adapted epitaxially to the Si(001) substrate. While, for samples formed from 0.1, 3.0 and 6.0 nm randomly shaped structures appeared.

The electrical characteristics in all samples are dominated by Fe-related defects in about 2 μm depth below the surface. The apparent doping concentration determined from the C-V characteristics decreases near the surface, the deep level defects compensate the doping of the starting wafer. The I-V and C-V characteristics in different junction has significant scatter, some of the junctions are dominated by leakage of the junctions in reverse bias. It is due to the rough silicides / silicon interface morphology and to very large defect concentration in the vicinity of the interface. The defect concentration measured by DLTS is an underestimation of the defect concentration since the filling pulses cannot fill defects in the whole depleted layer volume.

4. CONCLUSIONS

Iron silicide nanostructuress are grown by conventional Fe evaporation and subsequent annealing method on Si(001) substrate. The size distribution and shape of the formed islands depend on the initial thickness of evaporated iron. Initially thicker films produce bigger size iron silicide nanostructures. In case of 0.3-1.0 nm thick iron film rectangular and elongated nanoobjects form in square directions, while thicker films result randomly shaped silicide objects. The electrical characteristics in all samples are dominated by Fe-related defects.

ACKNOWLEDGEMENTS

The authors would like to thank the support of OTKA Grant No. 81998.

REFERENCES

1. T. Buonassisi, A.A. Istratov, M.A. Marcus, B. Lai, Z. Cai, S.M. Heald, E.R. Weber, *Nat. Mater.* **4**, 676 (2005).
2. S. Terasawa, T. Inoue, M. Ihara, *Sol. Energ. Mater. Sol. C.* **93**, 215 (2009).
3. N.E. Christensen, *Phys. Rev. B* **42**, 7148 (1990).
4. K. Yamaguchi, K. Mizushima, *Phys. Rev. Lett.* **86**, 6006 (2001).
5. G. Molnár, L. Dózsa, G. Pető, Z. Vértesy, A.A. Koós, Z.E. Horváth, E. Zsoldos, *Thin Solid Films* **459**, 48 (2004).
6. A.L. Barabási, *Appl. Phys. Lett.* **70,** 2565 (1997).
7. J. Tersoff, F.K. LeGoues: *Phys. Rev. Lett.* **72**, 3570 (1994).
8. N. Vouroutzis, T.T. Zorba, C.A. Dimitriadis, K.M. Paraskevopoulos, L. Dózsa, G. Molnár. *J. Alloy. Compd.* **448**, 202 (2008).
9. M. Zinke-Allmang, *Thin Solid Films* **346**, 1 (1999).